Si-CMOS-compatible lift-off fabrication of low-loss planar chalcogenide waveguides

Juejun Hu[1], Vladimir Tarasov[1], Nathan Carlie[2], Ning-Ning Feng[1], Laeticia Petit[2], Anu Agarwal[1*], Kathleen Richardson[2], and Lionel Kimerling[1]

[1]Microphotonics Center, Massachusetts Institute of Technology, Cambridge, Massachusetts 02139, USA
[2]Advanced Materials Research Laboratory, Clemson University, Anderson, South Carolina 29625, USA
**Corresponding author: anu@mit.edu*

Abstract: We demonstrate, for the first time to the best of our knowledge, low-loss, Si-CMOS-compatible fabrication of single-mode chalcogenide strip waveguides. As a novel route of chalcogenide glass film patterning, lift-off allows several benefits: leverage with Si-CMOS process compatibility; ability to fabricate single-mode waveguides with core sizes down to submicron range; and reduced sidewall roughness. High-index-contrast $Ge_{23}Sb_7S_{70}$ strip waveguides have been fabricated using lift-off with excellent uniformity of loss propagation and the lowest loss figure of reported to date. We also show that small core $Ge_{23}Sb_7S_{70}$ rib waveguides can be fabricated via lift-off as well, with loss figures lower than 0.5 dB/cm. Additionally, we find through waveguide modal analysis that although overall transmission loss is low, the predominant source of this loss comes from scattering at the sidewalls.

OCIS codes: (130.2790) Guided waves; (130.3120) Integrated optics devices; (130.3130) Integrated optics materials; (160.2750) Glass and other amorphous materials; (230.7390) Waveguides, planar; (310.1860) Deposition and fabrication.

References and links

1. P. Lucas, D. Le Coq, C. Juncker, J. Collier, D. Boesewetter, C. Boussard-Pledel, B. Bureau, M. Riley, "Evaluation of toxic agent effects on lung cells by fiber evanescent wave spectroscopy," Appl. Spectrosc. **59**, 1-9 (2005).
2. M. Asobe, H. Itoh, T. Miyazawa, and T. Kanamori, "Efficient and ultrafast all-optical switching using high Δn, small core chalcogenide glass fibre," Electron. Lett. **29**, 1966-1968 (1993).
3. C. Florea, J. Sanghera, L. Shaw, V. Nguyen, and I. Aggarwal, "Surface relief gratings in AsSe glass fabricated under 800-nm laser exposure," Mater. Lett. **61**, 1271-1273 (2007).
4. W. Chung, H. Seo, B. Park, J. Ahn, and Y. Choi, "Selenide glass optical fiber doped with Pr^{3+} for U-band optical amplifier," Etri J. **27**, 411-417 (2005).
5. O. Efimov, L. Glebov, K. Richardson, E. Van Stryland, T. Cardinal, S. Park, M. Couzi, and J. Bruneel, "Waveguide writing in chalcogenide glasses by a train of femtosecond laser pulses," Opt. Mater. **17**, 379-386 (2001).
6. N. Ponnampalam, R. DeCorby, H. Nguyen, P. Dwivedi, C. Haugen, and J. McMullin, "Small core rib waveguides with embedded gratings in As_2Se_3 glass," Opt. Express **12**, 6270-6277 (2004).
7. M. Veinguer, A. Feigel, B. Sfez, M. Klebanov, V. Lyubin, "New Application of Inorganic Chalcogenide Photoresists in Lift-off Photolitography," J. Optoelectron. Adv. Mater. **5**, 1361-1364 (2003).
8. C. Huang, D. Hewak, and J. Badding, "Deposition and characterization of germanium sulphide glass planar waveguides," Opt. Express, **12**, 2501-2506 (2004).
9. J. Frantz, L. Shaw, J. Sanghera and I. Aggarwal, "Waveguide amplifiers in sputtered films of Er^{3+}-doped gallium lanthanum sulfide glass," Opt. Express, **14,** 1797-1803 (2004).
10. J. Viens, C. Meneghini, A. Villeneuve, T. Galstian, E. Knystautas, M. Duguay, K. Richardson, and T. Cardinal, "Fabrication and characterization of integrated optical waveguides in sulfide chalcogenide glasses," J. Lightwave Technol. **17**, 1184-1191 (1999).
11. J. Hu, V. Tarasov, A. Agarwal, L. Kimerling, Microphotonics Center, Massachusetts Institute of Technology, 77 Mass Ave, Cambridge, M.A. 02139 and N. Carlie, L. Petit, K. Richardson are preparing a manuscript to be called "Exploration of Waveguide Fabrication From Thermally Evaporated Ge-Sb-S Glass Films."
12. Y. Ruan, W. Li, R. Jarvis, N. Madsen, A. Rode, and B. Luther-Davies, "Fabrication and characterization of low loss rib chalcogenide waveguides made by dry etching," Opt. Express **12**, 5140-5145 (2004).

#85531 - $15.00 USD Received 3 Aug 2007; revised 24 Aug 2007; accepted 27 Aug 2007; published 31 Aug 2007

13. R. DeCorby, N. Ponnampalam, M. Pai, H. Nguyen, P. Dwivedi, T. Clement, C. Haugen, J. McMullin, S. Kasap, "High index contrast waveguides in chalcogenide glass and polymer," IEEE J. Sel. Top. Quantum Electron. **11**, 539-546 (2005).
14. Y. Ruan, D. Freeman, N. Madsen, R. Jarvis, A. Rode, S. Madden, and B. Luther-Davies, "Fabrication and Characterization of Submicron Chalcogenide Waveguides," presented at the Conference on Optoelectronic and Microelectronic Materials and Devices, Brisbane, Australia, 8-10 Dec. 2004
15. L. Petit, N. Carlie, F. Adamietz, M. Couzi, V. Rodriguez, and K. C. Richardson, "Correlation between physical, optical and structural properties of sulfide glasses in the system Ge-Sb-S," Mater. Chem. Phys. **97**, 64-70 (2006).
16. J. Hu, V. Tarasov, N. Carlie, L. Petit, A. Agarwal, K. Richardson, and L. Kimerling, "Fabrication and Testing of Planar Chalcogenide Waveguide Integrated Microfluidic Sensor," Opt. Express, **15**, 2307 (2007).
17. D. Sparacin, S. Spector, and L. Kimerling, "Silicon Waveguide Sidewall Smoothing by Wet Chemical Oxidation," J. Lightwave Technol. **23**, 2455-2461 (2005).
18. W. Li, Y. Ruan, B. Luther-Davies, A. Rode, and R. Boswell, "Dry-etch of As2S3 thin films for optical waveguide fabrication," J. Vac. Sci. Technol. A **23**, 1626-1632 (2005).
19. C. Xu, W. Huang, M. Stern, and S. Chaudhuri, "Full-vectorial mode calculation by finite difference method," IEE Proc. Optoelectron. **141**, 281–286 (1994).
20. T. Barwicz and H. Haus, "Three-dimensional analysis of scattering losses due to sidewall roughness in microphotonic waveguides," J. Lightwave Technol. **23**, 2719-2732 (2005).

1. Introduction

Chalcogenide glasses (ChG's) have received considerable attention for applications in microphotonic devices in recent years due to their unique properties such as high infrared transparency, photosensitivity, large optical nonlinearity, capability of variations of properties and almost unlimited ability for doping and alloying. An array of fiber-based photonic devices such as fiber optical sensors [1], all-optical switches [2], surface gratings [3] and optical amplifiers [4], all of which utilize these unique properties of ChG's, have already been demonstrated. Compared to their fiber counterparts, microphotonic devices based on planar optical waveguides are mechanically more robust and are suitable for interfacing with other on-chip electronic and photonic devices. In addition, the possibility of significant cost reduction combined with the ability to take advantage of process improvements and economies of scale, all of which are enabled by leveraging on large-scale wafer processing, make planar chalcogenide based devices an attractive alternative over their fiber based counterparts.

To date, a number of patterning methods including direct laser writing [5], wet etching [6,7], dry etching [8] and lift-off [9] have been utilized for chalcogenide waveguide fabrication. While laser writing usually leads to waveguides with a typical low index contrast of 0.01, the latter three techniques are all applicable for high-index-contrast waveguide definition. Nevertheless, since chalcogenide glass films can be attacked by commercial (NH_4OH)-based developers, standard Si-CMOS photolithography often leads to pinhole formation and film peeling [10]. The yield of fabricated waveguides is low unless special photolithography and etching protocols [11], or even additional processing steps such as metal hard mask patterning [12], are employed. This complicates the fabrication process. Furthermore, at this time chalcogenide materials are not regarded as compatible with a standard Si-CMOS (Complementary Metal-Oxide-Semiconductor) process. Hence etch patterning techniques entail dedicated lithography and etching tools to avoid contamination in a CMOS foundry, which significantly increases the processing cost.

From previous studies, besides circumventing the processing difficulties encountered in chalcogenide waveguide fabrication, one key issue has always been waveguide transmission loss reduction. Our work focuses on the fabrication of high-index-contrast ($\Delta n>1$) chalcogenide waveguides. However, to date most work on high-index-contrast waveguides is based on the Silicon On Insulator (SOI) material system and investigations into chalcogenide waveguides are scarce. Towards this end, it is critical to understand the dominant source of optical loss in such waveguides. DeCorby, *et al*. studied wet-etch patterned As_2Se_3 strip waveguides with an estimated loss number of the order of 10 dB/cm and suggested that discrete fabrication defects arising from etchant undercut contributed significantly to

#85531 - $15.00 USD Received 3 Aug 2007; revised 24 Aug 2007; accepted 27 Aug 2007; published 31 Aug 2007

scattering loss [13]. Ruan, *et al*, reported the fabrication of submicron chalcogenide waveguides using contact printing and focused ion beam milling, which led to scattering from sidewall roughness as the dominant source of loss, although detailed waveguide loss data were not presented [14]. Despite the technical importance of high-index-contrast chalcogenide waveguides, the mechanism of optical loss in these waveguides is still open to investigation.

In this paper, we describe the use of the lift-off technique for fabrication of single-mode high-index-contrast $Ge_{23}Sb_7S_{70}$ waveguides, with maximized leverage on CMOS processing tools. Waveguide loss has been measured using fiber coupling and sidewall roughness has been evaluated using Atomic Force Microscopy (AFM). We also present the loss in strip waveguides and correlate it with the waveguide width and wavelength in order to identify the origin of optical loss in the investigated waveguides.

We have also demonstrated that low-loss (loss < 0.5 dB/cm at 1550 nm) rib waveguides can be fabricated by lift-off, a technique which yields waveguide devices with excellent uniformity over an entire 6" Si wafer. Optical loss in the as-fabricated strip waveguides has been determined to be 2-6 dB/cm at 1550 nm wavelength, the lowest loss figures reported to date in high-index-contrast submicron chalcogenide waveguides, to the best of our knowledge.

The entire fabrication process, except for chalcogenide deposition, has been carried out on a standard CMOS line. The amorphous nature of chalcogenide glasses eliminates the need for film growth on single-crystalline substrates, and hence allows backend CMOS compatibility. The advantage of this compatibility is two fold: it minimizes the need for dedicated facilities, thus significantly reducing device fabrication cost; and it enables fine-line patterning since we can leverage on existing CMOS processing facilities and its associated knowledge base. The fine-line lithography option allows the fabrication of two important classes of optical devices: monolithic low-power all-optical switches based on optical non-linear effects, and optical couplers that have stringent fabrication tolerance requirements. Additionally this submicron patterning capability facilitates microphotonic integration.

2. Device fabrication

2.1 Film deposition

Bulk $Ge_{23}Sb_7S_{70}$ glass is prepared from high purity elements using a traditional chalcogenide melt-quenching technique. From this bulk high-quality thin films are deposited onto substrates using thermal evaporation. Details of the bulk sample preparation and film deposition process may be found elsewhere [15, 16]. The thickness of the film was measured using a Tencor P10 surface profiler. Using a Metricon 2010 prism coupler, the refractive index of the as-evaporated film was determined to be (2.24 ± 0.02) at 1550 nm.

2.2 Waveguide fabrication

As in a standard lift-off process, a photoresist pattern is first formed on a substrate, which is a blank oxide-coated Si wafer in our case. $Ge_{23}Sb_7S_{70}$ is then thermally evaporated onto the wafer patterned with photoresist, and sonicated in solvent (usually acetone) to dissolve the photoresist layer beneath the undesired parts of the $Ge_{23}Sb_7S_{70}$ film, thus lifting it off. Only $Ge_{23}Sb_7S_{70}$ deposited onto areas not covered by photoresist is retained, and thus a chalcogenide pattern reverse that of the photoresist is defined. The patterned wafer is then rinsed in methanol and isopropanol to clean the surface. To fabricate rib waveguides, a second $Ge_{23}Sb_7S_{70}$ deposition is made sequentially on a lift-off patterned $Ge_{23}Sb_7S_{70}$ film. A schematic of the process flow is shown in Fig. 1(a) and the relevant waveguide dimensions in this study are illustrated in Fig. 1(b).

In our process, the starting substrates are 6" Si wafers already coated with a 3 μm-thick thermal oxide (Silicon Quest International Inc.). Commercially available negative resist NR9-1000PY (Futurrex Inc.) is used due to its negative-sloping sidewall profile and superior pattern resolution. The resist is spin-coated onto substrates on a manual photoresist coater (Model 5110, Solitec Inc.). UV exposure is carried out using a Nikon NSR-2005i9 i-line

#85531 - $15.00 USD Received 3 Aug 2007; revised 24 Aug 2007; accepted 27 Aug 2007; published 31 Aug 2007

wafer stepper (minimum linewidth 500 nm). Resist pattern development and subsequent baking are both completed on an SSI 150 automatic photoresist coater/developer track. The entire photolithography process is performed in a class-10 CMOS clean room in the Microsystems Technology Laboratory at MIT. No additional upper cladding layer is added for two reasons: first, in this study we would like to investigate optical properties that are intrinsic to chalcogenide glass films, so an upper cladding layer which can introduce additional loss due to cladding material absorption is avoided; second, air-cladded waveguide configuration is appropriate for applications such as chemical and biological sensing, in which direct interaction between the waveguide mode and external environment is necessary.

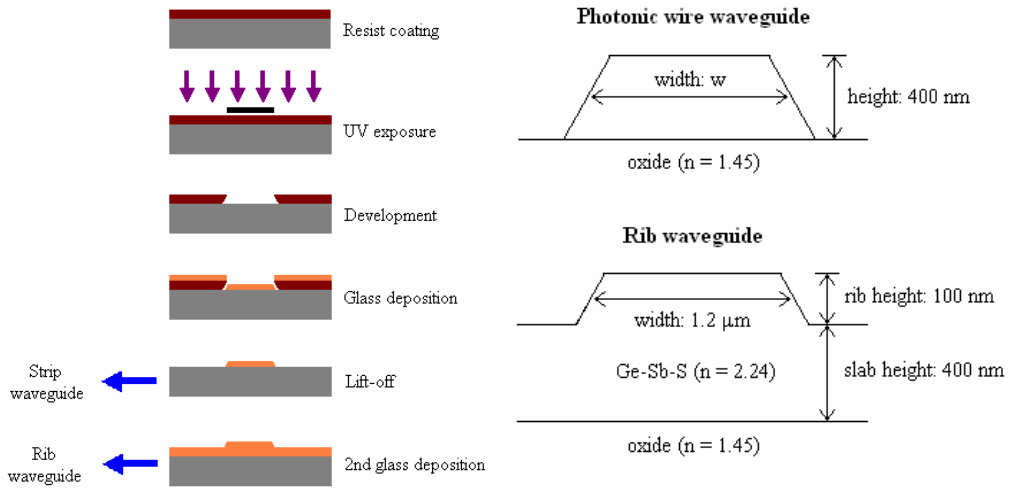

Fig. 1. (a). Schematic cross-sectional process flow of $Ge_{23}Sb_7S_{70}$ waveguide fabrication by lift-off; (b) Dimensions of fabricated $Ge_{23}Sb_7S_{70}$ strip and rib waveguides.

3. Device characterizations

3.1 Waveguide morphology

Morphology of $Ge_{23}Sb_7S_{70}$ waveguides is characterized using a JEOL 6320FV field-emission high-resolution SEM. A Digital Instruments Nanoscope IIIa Atomic Force Microscope (AFM) is used to measure the roughness of the as-patterned $Ge_{23}Sb_7S_{70}$ waveguides. AFM Measurement scans are performed parallel to the direction of the waveguides using the tapping mode, and the data obtained is analyzed using the Digital Instruments Nanoscope Software.

3.2 Waveguide loss measurement

$Ge_{23}Sb_7S_{70}$ waveguide transmission loss measurements are performed on a Newport AutoAlign workstation in combination with a JDSU SWS tunable laser. Lens-tip fibers are used to couple light from the laser into and out of the waveguides. Reproducible coupling between waveguides and fibers is achieved via an automatic alignment system with a spatial resolution better than 20 nm. Optical loss in strip waveguides is measured by a cutback method using paper-clip waveguide patterns, whereas rib waveguide loss is determined by traditional Fabry-Perot method considering the large bending loss in rib waveguides due to their small effective index contrast [17]. Finite-Difference Time-Domain (FDTD) technique is used to simulate the waveguide facet reflectivities for accurate determination of waveguide loss via the Fabry-Perot method. Each loss number reported in this paper is averaged over > 20 waveguides.

#85531 - $15.00 USD Received 3 Aug 2007; revised 24 Aug 2007; accepted 27 Aug 2007; published 31 Aug 2007

4. Results and discussion

The aim of our study is two-fold: to demonstrate lift-off as a novel route of chalcogenide glass film patterning for single-mode, high-index-contrast waveguide fabrication (core sizes are in the submicron range), and to identify the origin of optical loss in such waveguides.

4.1 Waveguide characterization

Figure 2(a) shows a cross-sectional SEM image of a strip $Ge_{23}Sb_7S_{70}$ waveguide before photoresist lift-off. Waveguides fabricated by lift-off typically show rounded corners, and the sidewall angle measured from the SEM image is ~ 65°. In our previous study [11], the sidewall angle measured was ~70°. The decrease of the sidewall angle in this work can be attributed to the new resist and exposure/developer tools used. Figure 2(b) shows the AFM scan of a 2 μm by 2 μm square area showing the surface morphology of a waveguide with a width of 750 nm. The AFM measurements also yield a sidewall line RMS roughness value of (11 ± 2) nm for as-fabricated waveguides, which is averaged over several AFM scans on different waveguides across an entire wafer, in good agreement with our previous study[11]. In comparison, plasma etched chalcogenide waveguide sidewalls exhibit RMS roughness values typically ranging from 20-150 nm depending on etching parameters [11, 18]. The relatively low sidewall roughness in waveguides fabricated through lift-off can be attributed to the fact that the sidewall is defined during a deposition process rather than etching. In the lift-off process, the major source of sidewall roughness probably originates only from edge roughness of photoresist patterns. Conspicuos by its absence here is the side-etching effect, often responsible for sidewall surface roughening in a standard etching process. We also find that waveguides with three different widths, 0.75 μm, 1.2 μm and 1.6 μm, exhibit the same sidewall roughness value within the accuracy of our AFM measurement. Similarly, the average RMS roughness on the strip waveguide top surface is determined to be (1.6 ± 0.3) nm, an understandably much lower value given that the top surface is formed during the film deposition process and is free of any roughness resulting from photolithography.

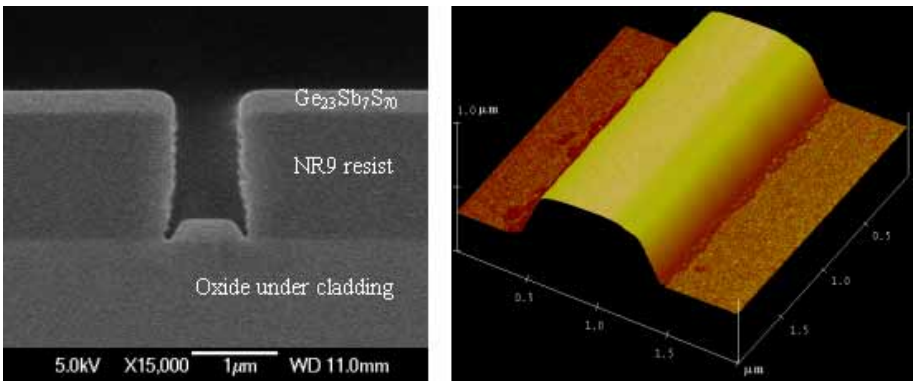

(a) (b)

Fig. 2. (a). Cross-sectional SEM image of a $Ge_{23}Sb_7S_{70}$ waveguide before photoresist lift-off, showing a sidewall angle of ~ 65° and rounded corners; (b) Submicron strip waveguide morphology measured by AFM with a sidewall RMS roughness value of (11 ± 2) nm and top surface RMS roughness of (1.6 ± 0.3) nm.

Measured transmission losses of strip and rib $Ge_{23}Sb_7S_{70}$ waveguides with different widths and cross-sectional geometry at the wavelength of 1550 nm are tabulated in Table 1, which shows that the Transverse-Magnetic (TM) mode exhibits lower transmission loss than the Transverse-Electric (TE) mode in strip waveguides with the same width. Also, transmission losses for both modes decrease as strip waveguides become wider. Additionally, as expected, the loss dependence on width is more significant for TE mode than for TM mode. All these experimental observations are characteristic of loss arising from sidewall roughness scattering, often the dominant loss mechanism in high-index-contrast waveguides, as we will

#85531 - $15.00 USD Received 3 Aug 2007; revised 24 Aug 2007; accepted 27 Aug 2007; published 31 Aug 2007

analyze in detail later. The rib waveguides show very low loss for both TE and TM modes due to less mode interaction with sidewall roughness in the rib waveguide geometry.

Table 1. Measured optical transmission losses and calculated modal parameters of $Ge_{23}Sb_7S_{70}$ waveguides at 1550 nm and modal parameters for fundamental TE/TM modes calculated using a finite-difference technique.

Waveguide width w	0.75 μm (strip)		1.2 μm (strip)		1.6 μm (strip)	1.2 μm (rib)
	TM	TE	TM	TE	TM	TE
Transmission loss (dB/cm)	3.9 ± 0.4	6.4 ± 0.8	3.5 ± 0.3	5.2 ± 0.5	2.3 ± 0.4	< 0.5
Number of modes supported	1	1	1	2	1	1
Effective index	1.602	1.721	1.660	1.848	1.674	1.987
Γ_{core}	0.966	0.726	0.767	0.980	0.783	0.989
$\Gamma_{surface}$ (nm^{-1})	6.00×10^{-3}	2.83×10^{-3}	3.07×10^{-3}	1.40×10^{-3}	1.69×10^{-3}	0.81×10^{-3}
$\Gamma_{sidewall}$ (nm^{-1})	4.80×10^{-3}	1.95×10^{-3}	1.74×10^{-3}	0.44×10^{-3}	0.33×10^{-3}	7.79×10^{-5}
$\alpha_{substrate}$ (dB/cm)	7.2×10^{-3}	0.098	2.8×10^{-5}	0.016	4.0×10^{-3}	2.8×10^{-4}

We also experimentally verified that loss of a strip waveguide is a function of wavelength, as is shown in Fig. 3. Transmission loss reduces for both TE and TM mode for longer wavelength.

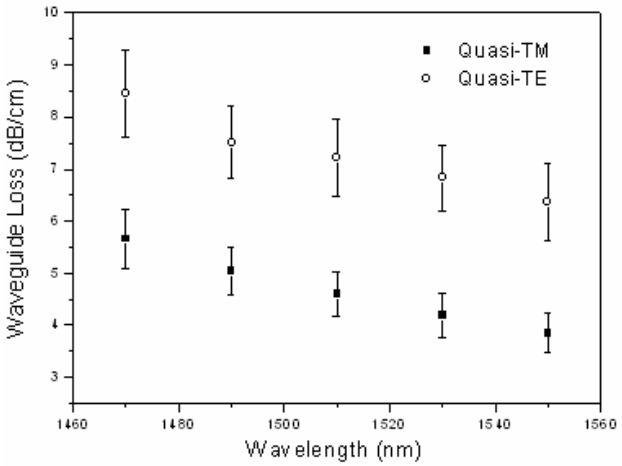

Fig. 3. Measured transmission loss of single-mode 0.75 μm × 0.4 μm $Ge_{23}Sb_7S_{70}$ strip waveguide as a function of wavelength. Loss increases for lower wavelength values, pointing to a negligible contribution from substrate leakage loss.

For practical applications we investigate the processing uniformity across an entire wafer. Towards this end, loss figures for 1.6 μm wide strip waveguides are measured using paper clip patterns on 40 different dies (waveguides with at least three different lengths are measured on each die to give one loss number) across a 6" wafer, and the distributions of waveguide loss values are shown in Fig. 4. Statistical analysis reveals that these waveguides have an average loss of (2.3 ± 0.4) dB/cm at 1550 nm wavelength. The small standard deviation of 0.4 dB/cm indicates excellent processing uniformity of our lift-off technique, and confirms that lift-off is intrinsically a wafer-scale processing technique and could be potentially scaled up for mass production.

#85531 - $15.00 USD Received 3 Aug 2007; revised 24 Aug 2007; accepted 27 Aug 2007; published 31 Aug 2007

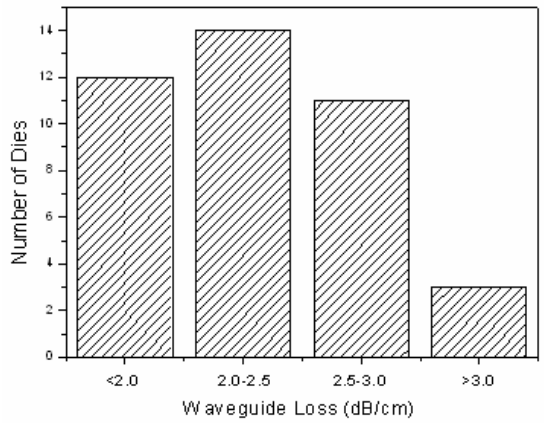

Fig. 4. Statistical distributions of loss values of 1.6 μm × 0.4 μm $Ge_{23}Sb_7S_{70}$ strip waveguides measured from 40 individual dies across a 6" wafer, which yield an average loss number of (2.3 ± 0.4) dB/cm. This tight distribution of waveguide loss values suggests excellent wafer-scale uniformity of the lift-off process.

4.2 Waveguide mode and loss analysis

Optical modes in strip $Ge_{23}Sb_7S_{70}$ waveguides are numerically simulated using a full-vectorial finite-difference method[19]. The simulated modes in both strip and rib waveguides are not rigorously pure TE or TM modes, and in the case of our lift-off defined waveguides, the coupling between TE and TM modes is enhanced due to the slanted sidewall profile. Figures 5(a) and 5(b) show, respectively, simulated quasi-TE and quasi-TM modal profiles for a 0.75 μm wide strip waveguide. The presence of both x and y in-plane electric field components for both TE and TM modes clearly indicates the mixed-polarization nature of the modes. For simplicity, we still refer to these quasi-TE/TM modes as TE/TM modes below.

#85531 - $15.00 USD Received 3 Aug 2007; revised 24 Aug 2007; accepted 27 Aug 2007; published 31 Aug 2007

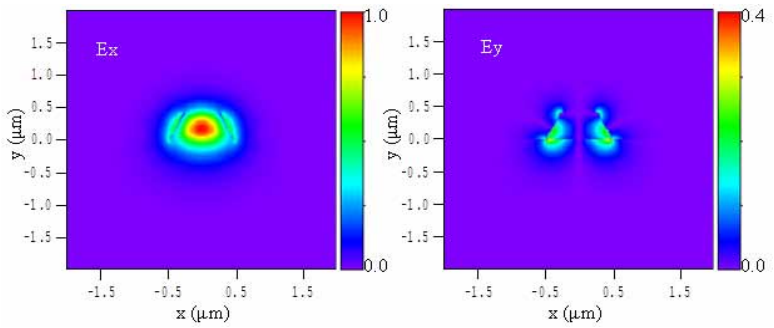

(a)

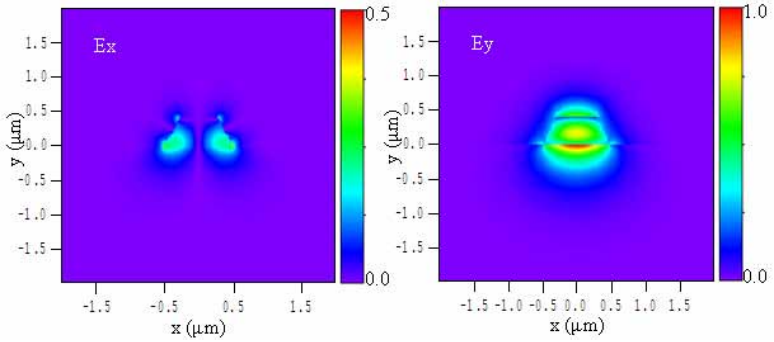

(b)

Fig. 5. Modal profiles of (a) quasi-TE mode and (b) quasi-TM mode in a 0.75 μm wide $Ge_{23}Sb_7S_{70}$ strip waveguide with 65° sidewall angle, simulated using a finite difference technique, indicating the mixed-polarization nature of the modes.

Generally, optical loss in waveguides is the sum of contributions from: bulk material absorption, scattering from top surface roughness, scattering from sidewall roughness, surface state absorption and optical power leakage into substrate, i.e. total transmission loss can be expressed as:

$$\alpha_{tot} = \sum \alpha = \alpha_{bulk\_absorption} + \alpha_{top\_roughness} + \alpha_{sidewall\_roughness} + \alpha_{surface\_absorption} + \alpha_{substrate} \quad (1)$$

For chalcogenide waveguide geometries shown in Fig. 1(b), the under cladding (thermal oxide) is transparent at 1550 nm wavelength and can be regarded as loss-less. Thus the only contribution of bulk material absorption comes from the $Ge_{23}Sb_7S_{70}$ core, which is given by:

$$\alpha_{bulk\_absorption} = \Gamma_{core}\alpha_{Ge_{23}Sb_7S_{70}} \quad (2)$$

where Γ_{core} represents modal power confinement factor in the $Ge_{23}Sb_7S_{70}$ core and $\alpha_{Ge23Sb7S70}$ is the bulk material absorption in $Ge_{23}Sb_7S_{70}$ film. Similarly, we can define the power confinement factor $\Gamma_{surface}$ near the waveguide surface, which is correlated to the surface absorption loss by:

$$\alpha_{surface\_absorption} = \Gamma_{surface}\alpha_{surface} \quad (3)$$

Note that here $\Gamma_{surface}$ denotes the optical power confined in a thin depth on the waveguide surface and thus has the dimension of inverse length (nm^{-1}). $\alpha_{sidewall\_roughness}$ and $\alpha_{top\_roughness}$ characterize the optical loss due to scattering and thus is a strong function of waveguide sidewall RMS roughness values and correlation length [20]. Contribution from scattering from top surface roughness is negligible, given the much smaller surface RMS roughness

#85531 - $15.00 USD Received 3 Aug 2007; revised 24 Aug 2007; accepted 27 Aug 2007; published 31 Aug 2007

measured by AFM. Therefore, Eq. (1) can be expressed as a linear combination from the different contributions:

$$\alpha_{tot} = \sum \alpha = \Gamma_{core}\alpha_{Ge_{23}Sb_7S_{70}} + \alpha_{sidewall\_roughness} + \Gamma_{surface}\alpha_{surface} + \alpha_{substrate} \quad (4)$$

Values of Γ_{core}, $\Gamma_{surface}$ and $\alpha_{substrate}$ for the waveguide geometries and modes in this study are calculated in a way similar to integrated the power flux density in the areas of interest and tabulated in Table 1. From Table 1 it is clear that substrate leakage ($\alpha_{substrate}$) hardly contributes to the waveguide loss due to the large index contrast between waveguide core and oxide under cladding. Low substrate leakage loss is also confirmed from Fig. 3, which shows that propagation loss in these waveguides increases rather than decreases at the shorter wavelengths. Another observation from Table 1 is that $\Gamma_{surface}$ is larger for TM modes compared to TE modes, which suggests that surface absorption is not the dominant source of loss since TE modes typically exhibit higher loss despite the smaller modal overlap with the waveguide surface. $\Gamma_{sidewall}$, defined in a way similar to that of $\Gamma_{surface}$ for optical field intensity near the waveguide sidewall, gives an estimate of the interaction strength between the optical mode and waveguide sidewall roughness. The very small values of $\Gamma_{sidewall}$ in rib waveguides indicate that optical loss in rib waveguides is solely induced by bulk and surface absorption. Thus the optical loss arising from bulk and surface absorption in strip waveguides can be extracted from rib waveguide loss figures using Eqs. (2) and (3). Since the TE mode confinement factor in the rib waveguide is close to unity, the upper limit of material loss in thermally evaporated $Ge_{23}Sb_7S_{70}$ films is thus ~ 0.5 dB/cm. Therefore, we conclude that optical loss in these high-index-contrast strip waveguides mainly arises from sidewall roughness scattering.

5. Conclusion

We demonstrate lift-off as a novel route for chalcogenide film patterning for single-mode, low loss strip and rib waveguide fabrication. The use of the lift-off technique allows leverage of CMOS facilities, which improves processing capabilities and projects significant cost reduction. In agreement with our previous work, the as-patterned lift-off waveguides exhibit a sidewall RMS roughness of (11 ± 2) nm, a smaller value compared to plasma-etch patterned waveguides. High-index-contrast single-mode $Ge_{23}Sb_7S_{70}$ strip waveguides have been fabricated using lift-off, with excellent wafer-scale uniformity and the lowest loss values (2-6 dB/cm) reported to date. Rib waveguide patterned by lift-off exhibits a low optical loss of < 0.5 dB/cm, indicating good chalcogenide film quality. Loss origins in high-index-contrast $Ge_{23}Sb_7S_{70}$ strip waveguides have been discussed based on detailed waveguide modal analysis resulting in the identification of sidewall roughness as the major source of optical loss in single-mode strip waveguides.

Acknowledgments

Funding support is provided by the Department Of Energy under award number DE-SC52-06NA27341. The authors would like to thank Mr. Rong Sun at MIT for technical assistance and helpful discussions. The authors also acknowledge the Microsystems Technology Laboratories at MIT for fabrication facilities and the Center for Materials Science and Engineering at MIT for characterization facilities.

Disclaimer

#85531 - $15.00 USD Received 3 Aug 2007; revised 24 Aug 2007; accepted 27 Aug 2007; published 31 Aug 2007

endorsement, recommendation, or favoring by the United States Government or any agency thereof. The views and opinions of authors expressed herein do not necessarily state or reflect those of the United States Government or any agency thereof.

#85531 - $15.00 USD Received 3 Aug 2007; revised 24 Aug 2007; accepted 27 Aug 2007; published 31 Aug 2007